VISUALIZING FLUID FLOW WITH MRI IN OIL-WET FRACTURED CARBONATE ROCK

Fernø, M.A.[1], Ersland, G.[1], Haugen, Å.[1], Graue, A.[1], Stevens, J.[2] and Howard, J.J.[2]
1) University of Bergen, Norway, 2) ConocoPhillips, USA

This paper was prepared for presentation at the International Symposium of the Society of Core Analysts held in Calgary, Canada, 10-12 September, 2007

ABSTRACT
The transfer of fluids from fractures into matrix and fracture fluid flow in oil-wet fractured limestone rocks was investigated experimentally using magnetic resonance imaging (MRI). Series of oil-water and water-oil displacements in stacked limestone core plugs were carried out at strongly water-wet and moderately oil-wet conditions, and the mechanisms of fluid flow into and across open fractures were determined as function of wettability and rock properties. A general-purpose commercial core analysis simulator was used to simulate the experimental results and investigate the controlling properties in fracture flow and fluid transport.

INTRODUCTION
Production of oil from naturally fractured reservoirs is commonly governed by interactions between gravity and co- and counter-current imbibition of water. Imbibition is dependent on wettability and the controlling capillary forces, and waterflooding fractured reservoirs have been successful in many water-wet reservoirs. Fractures generally exhibit a relatively small volume of the total porosity in fractured reservoirs (typically 1-3 %), but the fracture network is important for fluid flow from the higher permeability and the augmentation of accessible surface in which imbibition may occur.

Capillary continuity between isolated matrix blocks is recognized as favorable in fractured reservoirs dominated by gravity drainage. Capillary continuity across fractures in preferentially water-wet reservoirs increases the height of the continuous matrix column and reduces the amount of capillary trapped oil, while in preferentially oil-wet reservoirs it may increase ultimate recovery during gas assisted gravity drainage. In fractured reservoirs produced by viscous fluid displacement, establishing stable wetting phase bridges may contribute to added viscous pressure components over isolated matrix blocks, and may thus increase the oil recovery above the spontaneous imbibition potential as shown by Graue *et al.* (1999a and 2001) and Aspenes *et al.* (2002). Several authors have shown experimentally that vertical capillary continuity across fractures becomes important when gravity is the driving force including Horie *et al.* (1988), Firoozabadi and Hauge (1990) and Firoozabadi and Markeset (1992). Saidi (1987) introduced the idea of capillary continuity through stable liquid bridges. Labastie (1990) found that increased permeability of porous material in the fracture increased the ultimate recovery of oil during gravity drainage. Stones *et al.* (1992) concluded that the size of the contact area of

the porous material controlled the transmissibility of oil, hence the ability of the fracture to transport liquids. Firoozabadi and Markeset (1994) observed capillary continuity between isolated matrix blocks by liquid film drainage along non-porous spacers placed inside fractures, and by liquid bridging forming inside the fracture. They concluded that the film flow and the degree of fracture liquid transmissibility controlled the rate of production across a stacked matrix blocks.

Capillary continuity in waterfloods was more recently investigated by Graue *et al.* (2003) in horizontal fracture crossing studies in stacked moderately water-wet (MWW) chalk plugs, where stable liquid bridges were observed across open fractures. The wetting phase bridges increased the waterflood efficiency and were strongly dependent on fracture surface wettability. Aspenes (2007) showed that capillary continuity exerted a viscous pressure component through the bridges across the open fracture with no physical matrix contact, and increased oil recovery well above the spontaneous imbibition potential in each isolated matrix block. Rangel-German *et al.* (2006) showed experimentally how capillary continuity could occur in any direction in a fractured system, depending on the relative strengths of the capillary and Darcy terms in the flow equations. They injected fluids horizontally through large matrix blocks separated by a horizontal fracture. They concluded that capillary continuity was higher in narrow fractures, and argued that fracture capillary pressure was the dominant factor.

OBJECTIVES

The main objective was to determine if similar viscous displacement mechanisms observed in fractured chalk plugs at moderately water-wet conditions could be observed in a more heterogeneous limestone at moderately oil-wet conditions. The significance of local porosity heterogeneity and, in particular, wettability on capillary continuity across open fractures was investigated.

BACKGROUND

During waterflood in large scale (20cm x 10cm x 5cm) fractured chalk blocks it was observed that capillary continuity was strongly dependent on wettability. Viksund *et al.* (1999) and Graue *et al.* (1999) found that water displaced oil in a block-by-block manner at strongly water-wet conditions during waterflood, while the water crossed fractures at an earlier stage, apparently through capillary contacts, at the moderately water-wet conditions ($I_w - I_o \leq 0.65$). Graue *et al.* (2001) increased the spatial resolution by using MRI to investigate the nature of the capillary contact on smaller stacked core samples (1.5” diameter). They found that droplets of water were forming on the surface of the fracture separating the core plugs during waterfloods, creating bridges for early water transport into the outlet core. The process was wettability dependent as bridges formed at moderately water-wet conditions, while no such bridges were formed at strongly water-wet conditions. Aspenes *et al.* (2002) further investigated the bridging phenomena, and found that the number of bridges was dependent on the fracture width, the matrix wettability and the flow rate.

In this study the mechanisms for liquid bridging were investigated for a more heterogeneous limestone rock at both strongly water-wet and moderately oil-wet conditions. The level of porosity heterogeneity of the limestone was high compared to chalk, but still fairly homogeneous from core to core. MRI was utilized to investigate the significance of wettability on fluid flow inside a 1 mm open fracture between stacked core plugs and to determine the role of capillarity on the formation of wetting phase bridges.

Wettability was measured by the Amott-Harvey (A-H) method, and we use the term "drainage" if S_w is decreasing and "imbibition" if S_w is increasing, irrespective of wettability preference.

EXPERIMENTAL PROCEDURES

Core plugs were stacked horizontally and the space between the plugs constituted the fracture, held at constant aperture using spacers. Fluids were injected at a constant flow rate while obtaining saturation development in two orthogonal directions described in Figure 1B. The *in-situ* saturation development was monitored at each given wettability and flow rate. D_2O-brine was used as the water phase to distinguish between oil and water in the MRI since D_2O has zero nuclear spin and reveals no signal above the background level. Decane, used as the oil phase, was sensitive for magnetic resonance and appeared bright on the images.

The fracture was created within a single core plug, using a circular saw, to ensure a continuous and uniform wettability distribution. The wettability preference of the outcrop limestone was altered using an aging technique described in Graue *et al.* (1999b & 2002) and Aspenes *et al.* (2003). A fast hardening epoxy coating the stacked cores ensured fluid flow through the porous media, without any fluids bypassing the fracture. The epoxy coat was applied after the wettability alteration process (i.e. the core was saturated with fluids), but before the core was cut in two. Polyoxymethylene (POM) end pieces were mounted at the core faces to distribute fluids across the entire cross sectional area. The permanent confining of strong epoxy coat was capable of holding internal pressures of up to 8 bars. The epoxy setup represented an adaptable system with regard to fracture configuration and pressure measurements inside fractures. The epoxy coated core system while placed inside the MRI is illustrated in Figure 1A.

EXPERIMENTAL RESULTS

Mercury injection and low field NMR spectroscopy indicated pore throat heterogeneity in the limestone rock, where up to three distinct distributions were identified. Spontaneous imbibition production rates at strongly water-wet conditions suggested lower capillarity compared to chalk. The limestone A-H index measured at strongly water-wet conditions (0.8-0.9) was lower than expected (1.0), and could be explained by pore structure. Our interpretation suggested that a pore structure of poorly connected large pores and better connected small pores could trap oil in the larger pores during spontaneous imbibition,

which was mobilized during the subsequent waterflood.

The stability of the wettability preference in chalk after aging was earlier established by Aspenes *et al.* (2003), however it needed to be confirmed in limestone for the rock to be used in repeated experiments. The stability was tested with three subsequent A-H tests in two aged limestone cores with different ageing times, 10 and 6 days, respectively. Neither cores spontaneously imbibed any water after aging, and the wettability index was fairly reproducible for both 10 and 6 days of ageing and within experimental uncertainty for the latter case, see Table 1.

The impact of wettability on fracture fluid dynamics and transport was investigated with an analysis of MRI images during series of oil and water injections. To guide the reader, the fluid flow in Figure 2 and Figure 4 is from the inlet plug, behind the image plane, towards the reader and then out of the image plane, to enter the outlet plug.

Figure 2 shows the saturation development in the fracture during two waterfloods at different wettabilities. At strongly water-wet conditions ($I_w - I_o = 0.9$) in Figure 2A, the injected water displaced oil upwards by hydraulic filling with a smooth and horizontal fluid contact. No oil remained in the fracture. At moderately oil-wet conditions ($I_w - I_o = -0.4$) in Figure 2B, the water filled the fracture hydraulically similar to the water-wet case; however, droplets of oil remaining in the cross sectional area covered by the rising water were observed (Figure 2B, 666 min). With time, the oil droplets gradually decreased in number and size, yet some oil remained in the fracture throughout the test. Figure 3 shows the water saturation development, together with injection- and fracture pressure, during the waterflood at moderately oil-wet conditions. Initially, the matrix water saturation and pressures were constant (left of the first dashed vertical line) due to the dead volumes in the experimental setup. The injected water reached the inlet core at the first dashed vertical line (about 300 min into the test), and the injection pressure and the inlet core S_w increased accordingly. The measured pressure in the fracture and the outlet core S_w remained constant. The inlet core S_w increased linearly with the rate of injection until approaching S_{or} and the rate of displacement decreased. The increase in outlet core S_w occurred at the second vertical dashed line (about 700 min into the test) and coincided with two observations related to the fracture; (1) the maximum fracture water saturation was reached and (2) a distinct increase in fracture pressure. The oil droplets at the fracture surface identified by the transverse images (Figure 2B) inhibited the fracture to fully saturate with water during waterflood.

Figure 4 shows the saturation development in the fracture during two oilfloods at different wettabilities. At strongly water-wet conditions ($I_w - I_o = 0.9$) in Figure 4A, the oil emerged in the fracture at the top, rapidly displacing all the water downwards at the rate of injection. At moderately oil-wet conditions ($I_w - I_o = -0.4$) in Figure 4B, oil droplets formed in the cross sectional area of the fracture surface before the oil saturation front reached the fracture (Figure 4B, 163 min). The oil displaced water in the fracture from top to bottom, similar to the SWW case. However, droplets of oil remained at the fracture

surface in areas covered by water (Figure 4B, 452 min and 506 min). Figure 5 illustrates the water saturation development, together with injection- and fracture pressure, during the oilflood at moderately oil-wet conditions. The inlet core S_w decreased linearly until oil reached the fracture at the first vertical dashed line (about 350 min into the test), and the rate of displacement decreased. The outlet core S_w remained constant until the fracture S_o allowed transport of oil. This transport was quantified by the observed difference in outlet core S_w at the intersection between the horizontal and the second vertical dashed line in Figure 5, and decreased the outlet core S_w by a few percent in saturation. Although the transport of oil was small, it demonstrated a mechanistic difference compared to the waterflood at MOW in Figure 3, identified by two observations; (1) the time and difference in fracture S_w at which the outlet core S_w decreased, as the fluid transfer across the fracture occurred at low fracture S_o during oilflood, in contrast to the high (maximum) fracture S_w required to transport water during waterflood, and (2) the absence of pressure increase related to the change in outlet core saturation, indicated with the second vertical dashed line in Figure 6.

SIMULATIONS

The Sendra core analysis simulator software was implemented to better illustrate the mechanisms working during water- and oilfloods. One of the motivations behind the simulations was to test the applicability of conventional core analysis software to capture the experimentally observed fluid transport across the fracture. However, the unsteady-state experimental data available did not provide optimal input data to the estimate of matrix multiphase functions (such as the capillary pressure curve and the relative permeability curve). The history match was performed using the experimentally obtained average production and differential pressure data, which provided information about the relative permeability after breakthrough only. The low fluid production after breakthrough, 4-5 % of the entire saturation range, suggests a low level of confidence in the estimated multiphase functions. Sylte *et al.* (2004) found that several types of experiments should ideally be used as inputs to obtain high confidence in the estimated multiphase functions from the simulations. This implies that the correct multiphase functions may not have been established during history match, although a good agreement between experiments and simulations was obtained; it is possible to get history matching with different combinations of curves. Despite this, the simulations adequately illustrated the difference in fluid flow during water- and oilfloods.

Figure 6 demonstrates the high level of consistency between experimental values and simulated results both for the waterflood (left) and the oil injection (right). Pressure and average water saturation development generally exhibited an excellent match between experimental and simulated data in both experiments. The fracture multiphase functions were manually adjusted to capture average fracture fluid development and to account for the effect of gravity and buoyancy. The experimentally observed oil phase continuity across the fracture during oilflood was reproduced by assigning a slightly negative capillary pressure curve in the fracture. This approach is generally performed to account for any continuity in the matrix across the fracture, such as touching points in rough

fracture surfaces or when the fracture is partially filled with porous or non-porous material. However, in the current experimental setup, the fracture was explicitly held open with no matrix contact, and the oil transport was established by the growing oil droplets and the capillary attraction to oil of the outlet core. To describe the observed transport of oil during oilflood in the simulator, a straight, slightly negative ($P_c(S_w=1.0)$=-6kPa to $P_c(S_w=0)$=0kPa) capillary pressure curve was assigned to the fracture. The capillary pressure continuity across the fracture described the fluid transport and captured the fracture average saturation development acceptably. A straight curve was used for simplicity. A threshold value between -2 and -3 kPa was identified, below which the water was not displaced from the fracture during the oilflood. The fracture relative permeability influenced fluid flow within the fracture, but had little impact compared to the capillary pressure curve on fluid transport into the outlet core in this experimental design. Small adjustments to the fracture relative permeability curves were performed between the oilflood and the waterflood to better capture the average fluid saturation development in the fracture.

Figure 7 shows the *in-situ* water saturation profile development during fluid injection, and illustrates how frontal movements and fracture/matrix communication changed when injecting water compared to oil. During waterflood, a sharp water front observed (Figure 8, left and the fracture filled with water before transported into the outlet core. During oilflood, the front was disperse and oil transport into the outlet core occurred before the fracture was filled (Figure 8, right). The fracture capillary pressure curve was held constant in both flushes, while the relative permeability curve was slightly adjusted.

DISCUSSION

The controlling fracture crossing properties during waterfloods in moderately water-wet chalk discussed by Graue *et al.* (2003) are mechanistically similar to oilflooding a moderately oil-wet rock. Experiments in this study were designed to investigate the potential for creating horizontal capillary pressure continuity in the oil phase by forming oil droplets across open fractures in oil-wet rock, by injecting both oil and water to mobilize fluids. Equivalent fluid injections at strongly water-wet and at moderately oil-wet conditions in identical experimental setups isolated the effect from wettability on horizontal capillary continuity across the vertical, open fracture. The droplets of oil observed at the fracture surface at moderately oil-wet conditions altered fracture fluid flow compared to the SWW case.

The fluid dynamics inside the fracture during water injection at SWW (Figure 2a) was controlled by gravity and buoyancy, where the injected water displaced oil upwards with a horizontal fluid contact. The equivalent water injection at MOW conditions (Figure 2b) demonstrated the influence of wettability, where droplets of oil were observed at the fracture surface. The main fluid contact between the fluids was still horizontal; however, droplets of oil resided, due to favorable capillary forces and local porosity heterogeneity at the fracture surface below the rising oil-water contact. No change with respect to the fracture/outlet core fluid transport during waterflood was observed when changing the

wettability conditions. At MOW conditions water did not transport into the outlet core before the fracture was fully saturated (Figure 3), identified by the development of fracture and outlet core saturations and the need for the injected water to overcome the outlet core capillary threshold pressure to water.

During oil injection at SWW conditions (Figure 4a), oil displaced water in the fracture from the top and downwards with a smooth horizontal fluid contact. At MOW conditions (Figure 4b), oil droplets formed at the fracture surface ahead of the front during, altering the fluid interaction. In addition, the wetting affinity between the injection fluid and the fracture surface resulted in oil moving into the outlet core before the fracture was filled, identified in Figure 8. The large differences observed in fracture fluid flow and at the fracture surface when changing wettability conditions from strongly water-wet to moderately oil-wet illustrated the significance of wettability.

The oil droplets were observed at the fracture surface in both waterfloods and oilfloods at MOW conditions; however, no oil transport due to the droplets was observed during waterfloods. In addition, the droplets detached from the fracture surface during waterflood and moved upwards in the fracture due to buoyancy. The droplets ability to grow on the fracture surface is controlled by wettability, differential pressure and rock properties such as capillarity and surface roughness. The degree of capillarity is suggested by the production rates observed in the spontaneous imbibition curves at SWW. During comparable fracture crossing tests, the mechanistically similar process of waterflooding a moderately water-wet rock, chalk (a more capillary dominated rock at SWW compared to the investigated limestone) exhibited larger droplet growth and larger fluid transport due to the droplets. This indicates that the capillarity of the rock, which is directly linked to pore structure, is an important property controlling the effect of droplet growth, and on the fracture's ability to transport fluids. This is in agreement with the critical fracture width, defined by Sajadian and Danesh (1998), which is the maximum width to retain a stable liquid bridge. They argued that the process was controlled by physical properties of the fracture (such as roughness and aperture) and fluid properties such as density difference and interfacial tension.

The simulated results illustrated the differences in fluid saturation development in both matrix and fracture, and captured the fracture transport properties when injecting water compared to oil in the moderately oil-wet stacked cores. The experimentally observed transport of oil was captured by assigning capillary pressure continuity across the fracture, conventionally performed to account for matrix points contacting across the fracture. In our case, although there was no matrix contact across the fracture, the slightly oil-wet fracture capillary pressure curve adequately captured the early transport of oil during oilflood, and described the saturation development during waterflood.

ACKNOWLEDGEMENTS

Two of the authors are indebted for financial support to the Norwegian Research Council. The authors acknowledge Einar Ebeltoft at Reslab Integration with assistance during numerical simulations.

CONCLUSIONS

- The MRI images of fluid saturation development in stacked limestone illustrated two different transport mechanisms for fluids crossing an open fracture at different wettability conditions:
  - In oilfloods, 1) at strongly water-wet conditions, oil hydraulically filled the fracture from the top, 2) at moderately oil-wet conditions, oil crossed the fracture through capillary pressure contacts, corroborating mechanistically the results previously observed when waterflooding chalk at moderately water-wet conditions.
  - In waterfloods, 1) at strongly water-wet conditions, water hydraulically displaced oil in the fracture from the bottom, 2) at moderately oil-wet conditions, droplets of oil formed on the entire cross sectional area of the fracture but no transport of oil was observed.
- The observed oil droplets contributed to capillary pressure continuity across the fracture during oil injection. The forming of capillary pressure contacts was strongly dependent on wettability.
- Simulations successfully reproduced the development of average saturation observed during the experiments. Capillary pressure continuity across the open fracture with no matrix contact described the experimentally observed fluid transport during oilflood.

REFERENCES

Aspenes, E., Graue, A., Baldwin, B.A., Moradi, A, Stevens, J. and Tobola, D.P., "Fluid Flow in Fractures Visualized by MRI During Waterfloods at Various Wettability Conditions – Emphasis on Fracture Width and Flow Rate", paper SPE77338 presented at the SPE ATCE, San Antonio, TX, September 29 – October 2, 2002

Aspenes, E., Graue, A. and Ramsdal, J., "In situ wettability distribution and wetting stability in outcrop chalk aged in crude oil", *Journal of Petroleum Science and Engineering*, (2003),**39**, pp. 337-350.

Aspenes, E., "Wettability effects on oil recovery mechanisms in fractured chalk", PhD thesis, University of Bergen, Norway, Feb, 2007

Firoozabadi, A. and Hauge, J., "Capillary Pressure in Fractured Porous Media", *JPT* (1990), pp. 784-791

Firoozabadi, A. and Markeset, T., "An Experimental Study of Capillary and Gravity Crossflow in Fractured Porous Media", paper SPE24918 presented at the SPE ATCE, Washington, D.C, October 4-7, 1992

Firoozabadi, A. and Markeset, T., "Fracture-Liquid Transmissibility in Fractured Porous Media", *SPE Reservoir Engineering*, (Aug. 1994), pp. 201-207

Graue, A., Viksund, B.G., Baldwin, B.A and Spinler, E., "Large Scale Imaging of Impacts of

Wettability on Oil Recovery in Fractured Chalk", *SPE Journal*, (1999a), **4**,1, pp. 25-36
Graue, A., Viksund, B.G. and Baldwin, B.A., "Reproducible Wettability Alteration of Low-Permeable Outcrop Chalk", *SPE Res. Eng. And Eval.,(1999b)* **2**, 2, pp. 134-140.
Graue, A., Aspenes, E., Moe, R.W., Baldwin, B.A., Moradi, A., Stevens, J., and Tobola, D.P., "MRI Tomography of Saturation Development in Fractures During Waterfloods at Various Wettability Conditions", paper SPE71506 presented at the SPE ATCE, New Orleans, Louisiana, September 30-October 3, 2001
Graue, A., Aspenes, E., Bognø, T., Moe, R.W. and Ramsdal, J., "Alteration of wettability and wettability heterogeneity", *Journal of Petroleum Science and Engineering,*(2002), **33,** pp 3-17
Graue, A., Baldwin, B.A. and Aspenes, E., "Complementary imaging techniques applying NTI and MRI determined wettability effects on oil recovery mechanisms in fractured reservoirs", paper SCA2003-14 presented at the SCA, Pau, France, 2003
Horie, T., Firoozabadi, A. and Ishimoto, K., "Capillary Continuity in Fractured Reservoirs", paper SPE18282 presented at the SPE ATCE, Houston, TX, 1988
Labastie, A.: "Capillary Continuity Between Blocks of a Fractured Reservoir", paper SPE 20515 presented at the SPE ATCE, New Orleans, LA, 1990
Ragnel-German, E., Serhat, A. and Castanier, L., "Multiphase-flow properties of fractured porous media", *Journal of Petroleum Science and Engineering,* (2006), **51**, pp. 197-213
Saidi, A.M., "Reservoir Engineering of Fractured Reservoirs", TOTAL Edition Presse, Singapore (1987), pp. 527-549
Sajadian, V.A and Danesh, A.,"Laboratory Studies of Gravity Drainage Mechanisms in Fractured Carbonate Reservoirs – Capillary Continuity", paper SPE49497 presented at the 8th Abu Dhabi International Petroleum Exhibition and Conference, Abu Dhabi, U.A.E, October 11-14, 1998
Sendra Core Simulator v1.9 - User Manual
Stones, E.J., Zimmerman, S.A., Chien, C.V. and Marsden, S.S., "The Effect of Capillary Connectivity on Across Horizontal Fractures on Gravity Drainage From Porous Media", paper SPE24920 presented at the SPE ATCE, Washington, D.C, October 4-7, 1992
Sylte, A., Ebeltoft, E. and Petersen, E.B., "Simultaneous Determination of Relative Permeability and Capillary Pressure Using Data From Several Experiments", paper SCA2004-17 presented at the SCA, Abu Dhabi, U.A.E, October 5-9, 2004
Viksund, B.G., Graue, A., Baldwin, B., and Spinler,E., "Imaging of Waterflooding a Fractured Block of Outcrop Chalk", Proceeding at the 5th Chalk Research Symposium, Reims, France, October 7-9, 1999.

Table 1. The stability of altered wettability conditions in three times repeated Amott-Harvey tests.

Core #	# days	Iw	I_o	**1.A-H**	Iw	I_o	**2.A-H**	Iw	I_o	**3. A-H**
1	10	0	0.56	**-0.56**	0	0.48	**-0.48**	0	0.44	**-0.44**
2	6	0	0.21	**-0.21**	0	0.22	**-0.22**	0	0.23	**-0.23**

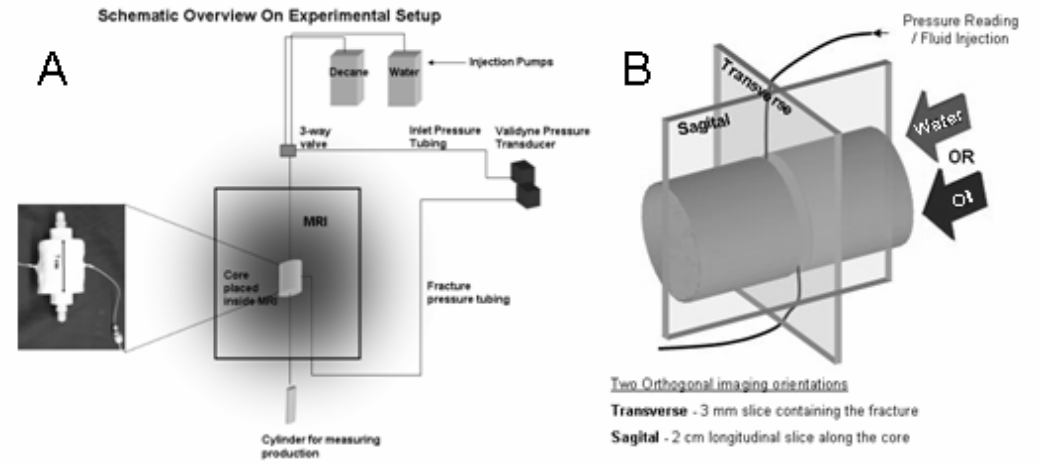

Figure 1. The MRI experimental setup with epoxy-coated core plug (A), and the orthogonal imaging direction with open vertical fracture and tubing inserted in the fracture (B).

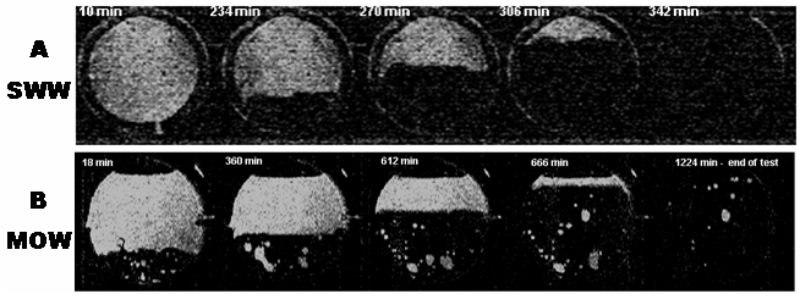

Figure 2. MRI images of saturation development in a 1mm wide fracture during waterflood at strongly water-wet (A: top) and moderately oil-wet (B: bottom) conditions.

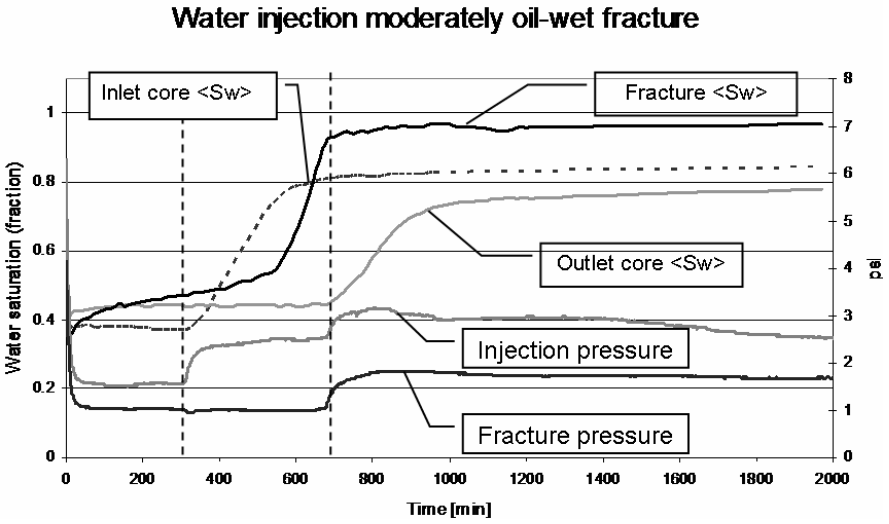

Figure 3. Development of saturation and pressure during waterflood at MOW conditions.

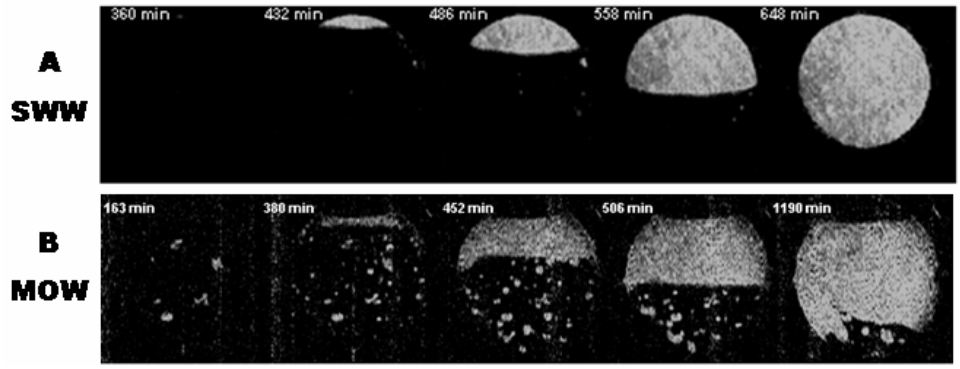

Figure 4. MRI images during oilflood at strongly water-wet (A: top) and moderately oil-wet (B: bottom) conditions.

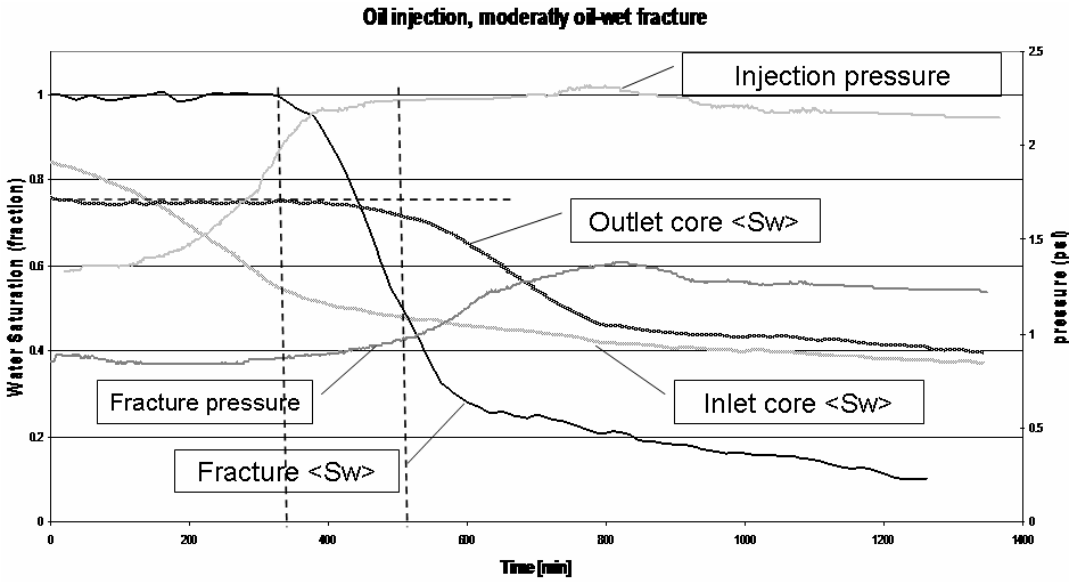

Figure 5. Development of saturation and pressure during oilflood at MOW conditions.

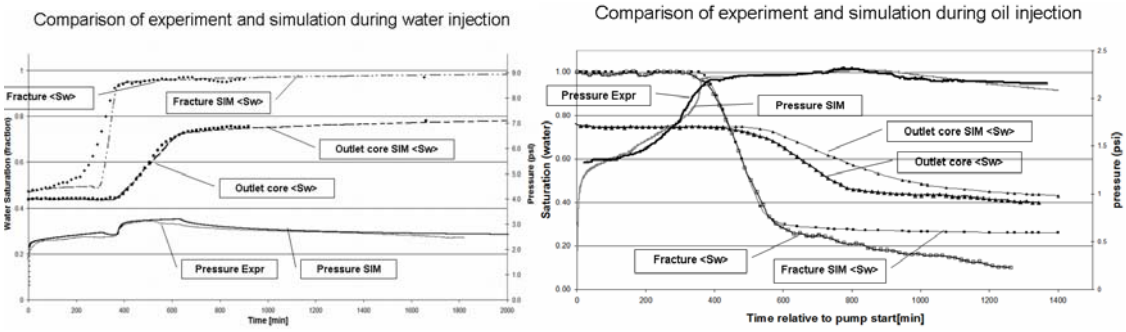

Figure 6. Comparison between experimental and simulated saturation and pressure development during the waterflood (left) and oil injection (right) at moderately oil-wet conditions.

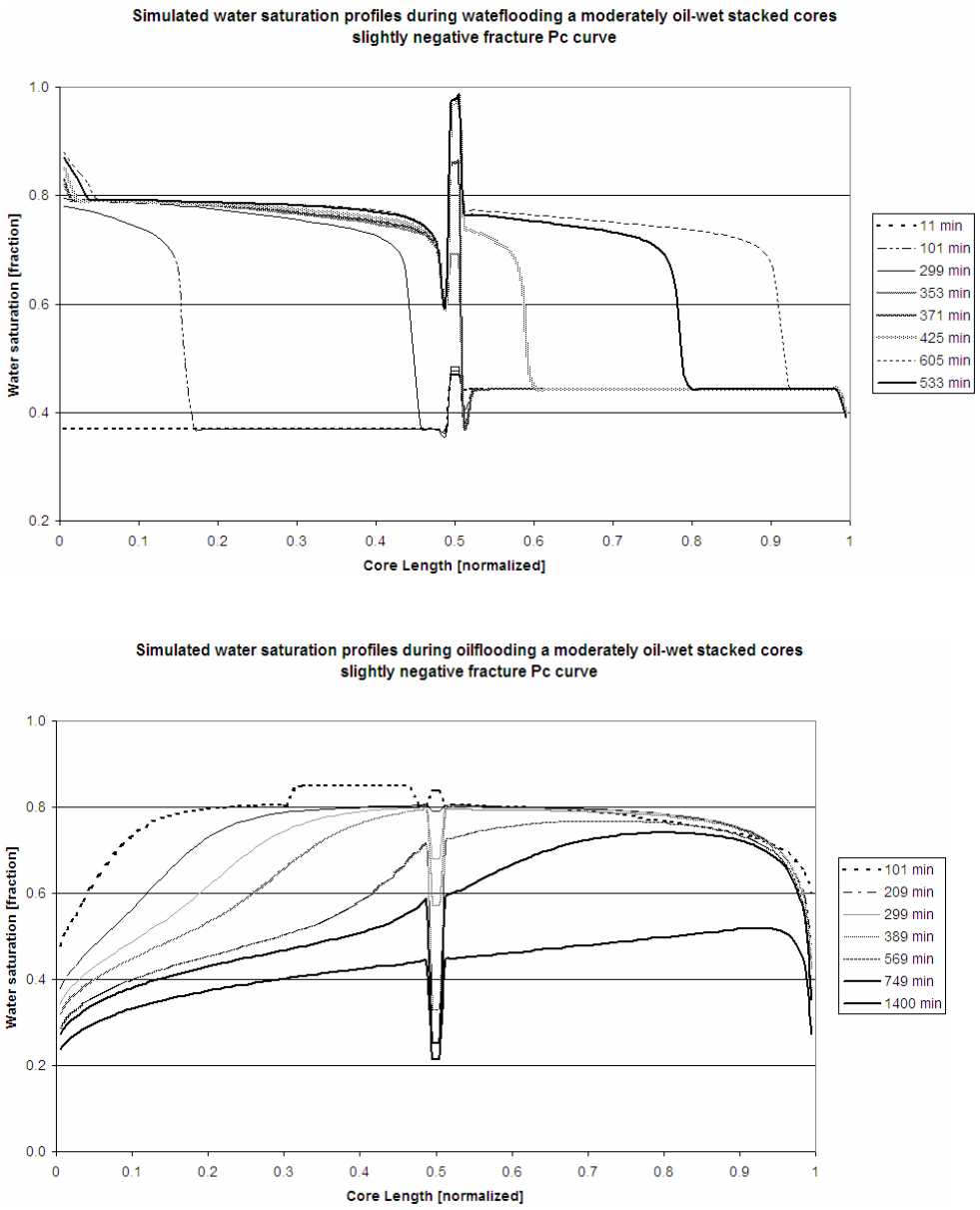

Figure 7. Simulated development of *in-situ* saturation profiles during waterflood (top) and oilflood (bottom) at moderately oil-wet wettability conditions. The fracture fills with water during waterflood before any water invades the outlet core. During oilflood, the oil invades the outlet core before the fracture is filled